NUMERICAL ANALYSIS OF HOMOJUNCTION GALLIUM ARSENIDE AVALANCHE PHOTODIODES (GAAS-APDS)

H. Mokari

Department of Electrical and Computer Engineering
Islamic Azad University
Science and Research Branch
Tehran, Iran

P. Derakhshan-Barjoei

Facility of Electrical Engineering
Islamic Azad University
Naein Branch
Naein, Iran

Abstract—In our earlier work we introduce a numerical analysis to investigate the excess noise and performance factor of double carrier multiplication homojunction avalanche photodiodes (APDs) considering the nonlocal nature of the ionization process. In this paper we investigate the gain, breakdown voltage and carrier injection breakdown probability of homojunction avalanche photodiode in the wide range of multiplication region width. Also in our calculations the effects of dead space has been considered. Our analyses based on the history dependent multiplication theory (HDMT) and width independent ionization coefficient.

1. INTRODUCTION

For high bit rate, long-haul fiber-optic communications, the avalanche photodiode (APD) is frequently the photodetector of choice owing to its internal gain, which provides a sensitivity margin relative to p-type-intrinsic-n-type (p-i-n) photodiodes. The multiplication region of an APD plays a critical role in determining the gain, the multiplication noise, and the gain-bandwidth product. According to the local-field avalanche theory [1–5], both the multiplication noise and the

gain-bandwidth product of APDs are determined by the ratio of the electron and hole ionization coefficients of the semiconductor in the multiplication region. Since this ratio is a material property, for a given electric field, efforts to improve the APD performance have focused on optimizing the electric field profile and characterizing new materials. Recently, lower multiplication noise and higher gain-bandwidth products have been achieved by sub micrometer scaling of the thickness of the multiplication region [4–12]. This is in direct contrast to what would have been predicted by the local-field model and is due to the nonlocal nature of impact ionization, which can be neglected if the thickness of the multiplication region is much greater than the "dead length", the distance over which carriers gain sufficient energy to impact ionize. However, when the dead space accounts for a significant portion of the multiplication region, the number of ionization chains that result in multiplication greatly in excess of the average gain is reduced, which, in turn, yields lower noise for a given gain. A similar noise suppression mechanism has been observed in mesoscopic conductors [13–15]. The minimum value to which the multiplication region can be scaled is ultimately determined by the onset of tunneling, which will result in excessive dark currents. In thick devices, the dead length comprises a small fraction of the multiplication region; hence, it can be ignored. On the other hand, when the thickness of the multiplication region is reduced to the point that it becomes comparable to a "few" dead lengths, the assumption of locality is no longer valid. In order to consider the nonlocal nature of impact ionization and accurately describe the avalanche process in thin layers, numerous analytical [16–18, 22] and numerical [23–27] techniques have been proposed. The numerical models that employ the Monte Carlo technique have the advantage of being formally exact, but their accuracy is frequently limited by the completeness of the band structure and the scattering models that are used in the simulation. In addition to being very computationally intensive, these models require several adjustable parameters to obtain adequate fits, thus obviating one of their advantages relative to analytical models. Recently, an analytical model that incorporates history-dependent ionization coefficients was developed and it was shown to provide excellent agreement with gain and noise measurements on GaAs APD's having multiplication layer thicknesses from 0.1 to 1.6 μm [28, 29].

One important aspect of the APD performance is the breakdown probability. Breakdown occurs when the APD's gain becomes infinite. In general, as the applied reverse-bias voltage is raised beyond a threshold, the probability that the gain becomes unstable diverges from zero, and gradually approaches unity as the voltage is further

raised. In fact, this threshold voltage is nothing but the breakdown voltage, which is defined as the applied reverse-bias voltage at which the *mean* gain becomes infinite. (Note that as the gain is integer-valued, its mean is finite if and only if the probability of having an infinite gain is zero.) The behavior of the breakdown probability, as a function of the applied revere-bias voltage, is the key indicator of how fast the transition from stable to saturated operation occurs. For example, when an APD is used in the Geiger mode, it is highly desirable that such a transition occur as rapidly as possible so that any incoming photon triggers a measurable response with near certainty. On the other hand, if the transition is not steep, then at any given applied reverse bias, a fraction of the absorbed photons (proportional to the complement of the breakdown probability) will fail to trigger breakdown, which reduces detection efficiency.

In 1999, McIntyre [7] adopted the recurrence principles developed by Hayat et al. [1, 14] and formulated recurrence equations which characterized the breakdown probability for the case of nonuniform fields.

Numerical analysis is efficient way to characterize the behavior of electrical devices [38–46]. In this paper, we will briefly review HDMT and introduce general numerical analysis to investigate the gain, breakdown voltage and carrier injection breakdown probability as well as carrier distributed breakdown probability of homojunction avalanche photodiode in the wide range of multiplication region width for GaAs-APDs. Also, we examine the effect of dead space on the characteristics of avalanche photodiodes in the wide range of multiplication region width. Our analysis based on the history dependent theory and width independent ionization coefficient.

2. THEORY REVIEW

This section reviews the gain, excess noise and performance factor calculation of the local-field theory and the history-dependent theory. The local-field theory assumes impact ionization is a continuous, whereas the history-dependent theory recognizes that the ionizing probability of a carrier depends on its history.

Throughout the calculations of this paper, we use a one-dimensional model and assume the n, i, and p regions are arrayed from left to right. The origin is at the interface of the n and i regions, and the thickness of the i region is ω. Thus, electrons are swept to the left and holes to the right [30].

2.1. The History-Dependent Theory

It is assumed that the carrier that starts impact ionization loses all of its energy relative to the band edge after each impact ionization event. In order to represent this process, history-dependent ionization coefficients $\alpha(x'|x)$ and $\beta(x'|x)$ are defined to represent the local ionization probability density at x for a carrier generated at x'. If an electron generated at x' can survive until it gets to x without ionizing, then the probability for it to ionize in the distance element dx is $\alpha(x'|x)$. The ionization probability of this electron $p_e(x'|x)$ in dx thus depends on the electron survival rate $P_{se}(x'|x)$. The survival rate and ionization probability of holes are defined similarly [30].

To calculate both the gain and noise, we utilize iterative technique. We can calculate the ensemble averages $N_e(x)$ and $N_h(x)$, the average numbers of the carriers in the two chains generated by the initial electron and hole injected at x separately. Since, in each ionization event the extra electron and hole are always generated in pairs, the final number of the electrons in the chain started by the initial pair is equal to that of the holes. The current gain is defined as the ratio of the number of final $e - h$ pairs to that of the injected $e - h$ pairs. So, the gain due to the initial pair injected at x' is [30]

$$M(x') = \frac{N_e(x') + N_h(x')}{2} \tag{1}$$

Since the noise power spectral density is proportional to the ensemble average $< n^2 >$, the calculation of noise starts from $< n_e^2 >$ and $< n_h^2 >$ for an electron-hole pair injected at x'. Considering all the ionization probabilities for the initial pair and assuming that the carriers are uncorrelated, i.e., $< n_x n_y > = < n_x > < n_y >$, $< n_e^2 >$ and $< n_h^2 >$ can be expressed as in [29]. Once $N_e(x)$ and $N_h(x)$ are solved in the gain calculation, $< n_e^2 >$ and $< n_h^2 >$ can be calculated similarly. Then, the excess noise factor of a δ injection at x' is given by the expression [30]

$$
\begin{aligned}
F(x') &= \frac{< m_e^2(x') >}{M^2(x')} = \frac{< \left(\dfrac{N_e(x') + n_h(x')}{2} \right)^2 >}{M^2(x')} \\
&= \frac{< n_e^2(x') > + < n_h^2(x') > + 2N_e(x')N_h(x')}{4M^2(x')}
\end{aligned}
\tag{2}
$$

2.2. General Injection Profile

In the local-field theory and the history-dependent theory, the following assumptions are implicit.

1) There is no interaction between any of the carriers in the multiplication region except at the moment of impact ionization.

2) There is no correlation between any carriers, and they contribute to noise independently. Thus, their noise spectral density can be added linearly.

These assumptions are quite reasonable for low-level injection, which is the common operating condition for most APD's. Assumption 1 also insures a linear response to injection. According to this assumption, the gain M_g for an arbitrary injection $g_0(x)$ can be written as a weighted average of the gain of each δ injection, which yields [30]

$$M_g = \frac{I}{I_0} = \frac{\displaystyle\int_0^\omega dx'[g_0(x')M(x')]}{\displaystyle\int_0^\omega dx'[g_0(x')]} \tag{3}$$

$$I_0 = \int_0^\omega dx'[g_0(x')]$$

where I_0 is the total injected current, and $M(x)$ is defined in (1) for the local-field theory and in (4) for the new theory. Similarly, according to Assumption 2, the current noise spectral density S for an arbitrary injection profile $g_0(x)$ is [30]

$$S = 2e\int_0^\omega dx'[g_0(x')M^2(x')f(x')]$$

$$R(\omega) = 2eI_g M_g^2 F_g R(\omega)$$

$$F_g = \frac{\displaystyle\int_0^\omega dx'[g_0(x')M^2(x')F(x')]}{M_g^2 \displaystyle\int_0^\omega dx' g_0(x')} \tag{4}$$

where $F(x)$ is defined in (2) for the local-field theory and in (5) for the history-dependent theory. F_g, which is a weighted average of $F(x)$, is the measured excess noise factor according to either theory.

2.3. Breakdown Probabilities for Thin Avalanche Photodiodes

Suppose that an electron is generated at location x within the multiplication region. Let $X_e(x)$, called the electron life span at x, be the random distance at which impact ionization occurs. Similarly, let $X_h(x)$, called the hole life span at x, be the random distance that

a hole, generated at location x, travels before it ionizes. The family of random variables $X_e(x)$ and $X_h(x)$ are assumed to be statistically independent for all $x \in [0, W]$ and to have probability density functions (pdfs) $h_e(x)$ and $h_h(x)$, respectively. These pdfs take the following form [34]:

$$h_e(x, \eta) = \begin{cases} 0 & \eta < d_e(x) \\ \alpha(\eta+x) \exp\{-\int\limits_{d_e(x)}^{\eta} \alpha(x+\sigma)d\sigma\} & d_e(x) \leq \eta \leq W - x \end{cases} \quad (5)$$

$$h_h(x, \eta) = \begin{cases} 0 & \eta < d_h(x) \\ \beta(\eta + x) \exp\{-\int\limits_{d_h(x)}^{\eta} \beta(x - \sigma)d\sigma\} & d_e(x) \leq \eta \leq x \end{cases} \quad (6)$$

Since our analysis is restricted to the multiplication region, the value of the pdfs for electrons h_e and holes h_h outside the multiplication region is not relevant.

Where d_e and d_h are dead space associated with a carrier born at x and α and β are the nonlocalized position-dependent ionization coefficient of electrons and holes, which can be calculated from the electric field through a material-dependent parametric model. Upon ionization, two electrons and a hole with zero initial kinetic energy are generated.

With the history-dependent probability densities we can write [37]:

$$P_{nbe}(x') = P_{se}(x'|0) + \int\limits_{0}^{x'} p_e(x'|x)P_{nbe}^2(x)P_{nbh}(x)dx \quad (7)$$

$$P_{nbh}(x') = P_{sh}(x'|\omega) + \int\limits_{0}^{\omega} p_h(x'|x)P_{nbh}^2(x)P_{nbe}(x)dx \quad (8)$$

The first of these equations states that if a cold electron is injected (created) at x', no breakdown occurs if 1) it manages to escape with no ionizations (P_{se}) or 2) if it does have a first ionization at x with a probability $p_e(x'|x)$, all three resulting cold carriers (two electrons and one hole), escape without initiating a breakdown. The second equation is an equivalent expression for holes. These expressions can be solved by successive iterations. It was found that the convergence is fairly slow close to the breakdown voltage but rapid well above the breakdown voltage.

3. RESULTS AND DISCUSSION

In the previous section we have introduced the theoretical background to determine the mean gain, breakdown voltage and breakdown probability excess of homojunction APDs. To see the effects of dead space on the characteristics of avalanche photodiodes we use the nonlocalized ionization coefficient model (width independent ionization coefficient) were taken from [31] and HDMT introduce in the previous section to characterize the behavior of the homojunction GaAs-APDs. In our calculations, we assumed a constant electric field profile within the multiplication region and used the simple approximation $V = \varepsilon W$ for the reverse bias voltage.

The mean gain as a function of the bias is depicted for the GaAs-APDs in Fig. 1. The plots are compared with the plots obtained using the theory with no dead space. In this latter case, the electron and hole ionization coefficients are taken to be the inverse of the electron and hole mean scattering distances, respectively.
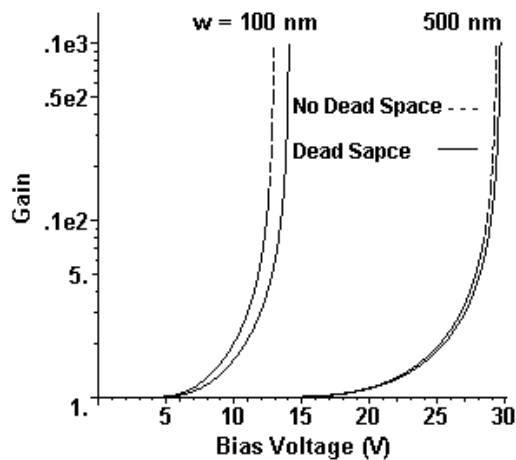
Figure 1. Comparison of the mean gain calculated with the local-field theory (dashed lines) and the history-dependent theory (solid lines) for GaAs-APDs.

It is seen that dead space reduces the mean gain. This effect is more significant for the thin APDs. This result resembles the result obtained for the case of uniform electric fields for which the reduction in mean gain due to dead space was more evident for APD's operating in the linear mode. The breakdown electric field as a function of the multiplication region is depicted for the GaAs-APDs in Fig. 2. As

shown in this figure the dead space cause to increase the predicted breakdown electric filed. Also as we can see, the effect of dead space decreases through the increases of multiplication region width.
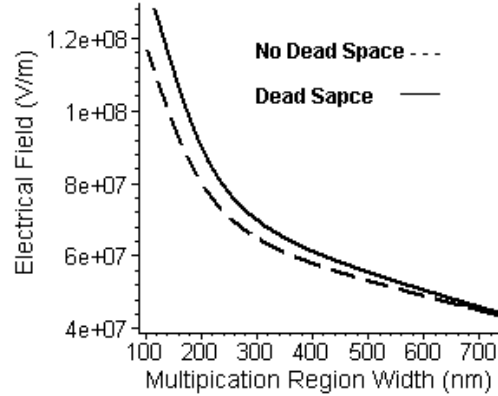
Figure 2. Comparison of the breakdown electric filed calculated with the local-field theory (dashed lines) and the history-dependent theory (solid lines) for GaAs-APDs.

Dead space also affects the breakdown probability of APDs. To see the roles of the multiplication-region width on the breakdown characteristics, we numerically computed the breakdown probability as a function of the applied reverse-bias voltage for GaAs and plotted n Fig. 3. Two sets of results were generated for each width. In the first set, we considered the dead space effects and in the second set of results we did not consider the dead space effects. The dead space decreases the probability of the initial impact ionization occurring in the onset of the multiplication process. This, in turn, will decrease the breakdown probability as each of the offspring electrons will have a lower chance of breakdown as they have a longer distance to travel. Note that the breakdown voltage is the voltage corresponding to the point when the breakdown probability begins to exceed zero. We also note that the calculated values of the breakdown probability near breakdown are sensitive to precision error (resulting from discretizing the recurrence equations); however, the calculated values rapidly stabilize beyond the breakdown voltage. We emphasize that in our calculation we used nonlocalized ionization coefficients. The use of the bulk, or so-called localized, ionization coefficients cannot be justified for our technique, as they are not consistent with the dead space theory. It was observed that attempting to use such localized coefficients in the current recurrence technique can lead to unstable solutions.
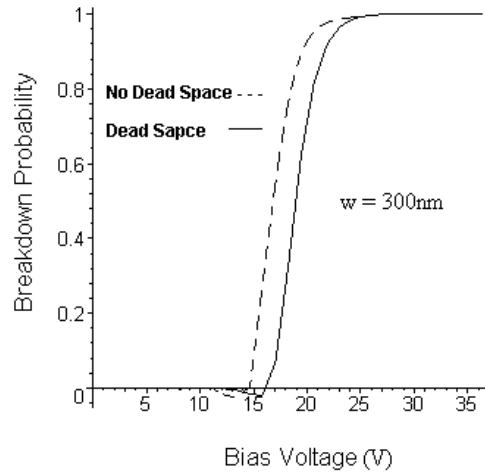
Figure 3. Comparison of the breakdown probability as a function of bias voltage calculated with the local-field theory (dashed lines) and the history-dependent theory (solid lines) for GaAs-APDs.

4. CONCLUSION

In this paper we were rigorously analyzed the characteristics of homojunction avalanche photodiodes by considering the effect of dead space. We have shown that the characteristics of APDs are affected not only by multiplication material but also by multiplication region width. Also we have found that the multiplication region width has a strong effect on the dead space and this effect for the thin APDs is more important than the thick APDs. Reducing the width of the multiplication layer serves to both downshift and sharpen the breakdown probability curve as a function of the applied reverse-bias voltage. Also, we showed that the breakdown characteristics are enhanced in thin APDs. In particular, reducing the thickness of the multiplication region not only serves to reduce the breakdown voltage but it also makes the transition from sub-breakdown to breakdown more abrupt on an absolute scale (the transmission abruptness relative to the breakdown voltage is reduced, however). This feature is particularly desirable for Geiger-mode operation of the APD, as the likelihood of breakdown is enhanced, which leads to enhanced detection and less sensitivity to bias fluctuations. Moreover, the absolute and relative abruptness of the transition can be further enhanced if injected photo generated carriers have an initial energy comparable to the ionization threshold.

REFERENCES

1. McIntyre, R. J., "Multiplication noise in uniform avalanche diodes," *IEEE Trans. Electron Devices*, Vol. ED-13, No. 1, 164–168, Jan. 1966.

2. Kagawazadeh, K., "The distribution of gains in uniformly multiplying avalanche photodiodes: Theory," *IEEE Trans. Electron Devices*, Vol. ED-19, 703–713, June 1972.

3. Emmons, R. B., "Avalanche-photodiode frequency response," *J. Appl. Phys.*, Vol. 38, No. 9, 3705–3714, 1967.

4. Campbell, J. C., S. Chandrasekhar, W. T. Tsang, G. J. Qua, and B. C. Johnson, "Multiplication noise of wide-bandwidth InP/InGaAsP/In-GaAs avalanche photodiodes," *J. Lightwave Technol.*, Vol. 7, 473–477, Mar. 1989.

5. Tarof, L. E., J. Yu, R. Bruce, D. G. Knight, T. Baird, and B. Oosterbrink, "High-frequency performance of separate absorption grading, charge, and multiplication InP/InGaAs avalanche photodiodes," *IEEE Photon. Technol. Lett.*, Vol. 5, 672–674, June 1993.

6. Hu, C., K. A. Anselm, B. G. Streetman, and J. C. Campbell, "Noise characteristics of thin multiplication region GaAs avalanche photodiodes," *Appl. Phys. Lett.*, Vol. 69, No. 24, 3734–3736, 1996.

7. Ong, D. S., K. F. Li, G. J. Rees, G. M. Dunn, J. P. R. David, and P. N. Robson, "A Monte Carlo investigation of multiplication noise in thin p-i-n GaAs avalanche photodiodes," *IEEE Trans. Electron Devices*, Vol. 45, 1804–1810, Aug. 1998.

8. Li, K. F., D. S. Ong, J. P. R. David, G. J. Rees, R. C. Tozer, P. N. Robson, and R. Grey, "Avalanche multiplication noise characteristics in thin GaAs p-i-n diodes," *IEEE Trans. Electron Devices*, Vol. 45, 2102–2107, Oct. 1998.

9. Li, K. F., S. A. Plimmer, J. P. R. David, R. C. Tozer, G. J. Rees, P. N. Robson, C. C. Button, and J. C. Clark, "Low avalanche noise characteristics in thin InP p-i-n diodes with electron initiated multiplication," *IEEE Photon. Technol. Lett.*, Vol. 11, 364–366, 1999.

10. Lenox, C., P. Yuan, H. Nie, O. Baklenov, C. Hansing, J. C. Campbell, and B. G. Streetman, "Thin multiplication region InAlAs homojunction avalanche photodiodes," *Appl. Phys. Lett.*, Vol. 73, 783–784, 1998.

11. Lenox, C., H. Nie, P. Yuan, G. Kinsey, A. L. Holmes, Jr., B. G. Streetman, and J. C. Campbell, "Resonant-cavity

InGaAs/InAlAs avalanche photodiodes with gain-bandwidth-product of 290 GHz," *IEEE Photon. Technol. Lett.*, Vol. 11, 1162–1164, Sept. 1999.

12. Gonzalez, T., C. Gonzalez, J. Mateos, D. Pardo, L. Reggiani, O. M. Bulashenko, and J. M. Rubi, "Universality of the 1/3 shot-noise suppression factor in nondegenerate diffusive conductors," *Phys. Rev. Lett.*, Vol. 80, No. 13, 2901–2904, 1998.

13. Reklaitis, A. and L. Reggiani, "Monte Carlo study of shot noise suppression," *J. Appl. Phys.*, Vol. 82, No. 6, 3161–3163, 1997.

14. Starikov, E., P. Shiktorov, V. Gruzinskis, L. Varani, J. C. Vaissiere, J. P. Nougier, T. Gonzalez, J. Mateos, D. Pardo, and L. Reggiani, "Transfer impedance calculations of electronic noise in two-terminal semiconductor structures," *J. Appl. Phys.*, Vol. 83, No. 4, 2052–2066, 1998.

15. Marsland, J. S., "On the effect of ionization dead spaces on avalanche multiplication and noise for uniform electric field," *J. Appl. Phys.*, Vol. 67, 1929–1933, 1990.

16. Hayat, M. M., B. E. A. Saleh, and M. C. Teich, "Effect of dead space on gain and noise of double-carrier-multiplication avalanche photodiodes," *IEEE Trans. Electron Devices*, Vol. 39, 546–552, 1992.

17. Hayat, M. M., W. L. Sargent, and B. E. A. Saleh, "Effect of dead space on gain and noise in Si and GaAs avalanche photodiodes," *IEEE J. Quantum Electron.*, Vol. 28, 1360–1365, 1992.

18. Marsland, J. S., R. C. Woods, and C. A. Brownhill, "Lucky drift estimation of excess noise factor for conventional avalanche photodiodes including the dead space effect," *IEEE Trans. Electron Devices*, Vol. 39, 1129–1134, 1992.

19. Okuto, Y. and C. R. Crowell, "Ionization coefficients in semiconductors: A nonlocal property," *Phys. Rev. B*, Vol. 10, 4284–4296, 1974.

20. Spinelli, A. and A. L. Lacaita, "Mean gain of avalanche photodiodes in a dead space model," *IEEE Trans. Electron Devices*, Vol. 43, 23–30, 1996.

21. Shichijo, H. and K. Hess, "Band-structure-dependent transport and impact ionization in GaAs," *Phys. Rev. B*, Vol. 23, 4197–4207, 1981.

22. Brennan, K. F., "Calculated electron and hole spatial ionization profiles in bulk GaAs and superlattice avalanche photodiodes," *IEEE J. Quantum Electron.*, Vol. 24, 2001–2006, 1988.

23. Sano, N. and A. Yoshii, "Impact-ionization theory consistent with

a realistic band structure of silicon," *Phys. Rev. B*, Vol. 45, 4171–4180, 1992.

24. Bude, J. and K. Hess, "Thresholds of impact ionization in semiconductors," *J. Appl. Phys.*, Vol. 72, 3554–3561, 1992.

25. Chandramouli, V. and C. M. Maziar, "Monte Carlo analysis of bandstructure influence on impact ionization in semiconductors," *Solid State Electron.*, Vol. 36, 285–290, 1993.

26. Kamakura, Y., H. Mizuno, M. Yamaji, M. Morifuji, K. Tanighchi, C. Hamaguchi, T. Kunikiyo, and M. Takenaka, "Impact ionization model for full band Monte Carlo simulation," *J. Appl. Phys.*, Vol. 75, 3500–3506, 1994.

27. Dunn, G. M., G. J. Rees, J. P. R. David, S. A. Plimmer, and D. C. Herbert, "Monte Carlo simulation of impact ionization and current multiplication in short GaAs p in diodes," *Semicond. Sci. Technol.*, Vol. 12, 111–120, 1997.

28. Ong, D. S., K. F. Li, G. J. Rees, J. P. R. David, and P. N. Robson, "A simple model to determine multiplication and noise in avalanche photodiodes," *J. Appl. Phys.*, Vol. 83, 3426–3428, 1998.

29. Spinelli, A., A. Pacelli, and A. L. Lacaita, "Dead space approximation for impact ionization in silicon," *Appl. Phys. Lett.*, Vol. 68, 3707–3709, 1996.

30. Yuan, P., K. A. Anselm, C. Hu, H. Nie, C. Lenox, A. L. Holmes, B. G. Streetman, J. C. Campbell, and R. J. McIntyre, "A new look at impact ionization — Part II: Gain and noise in short avalanche photodiodes," *IEEE Trans. Electron Devices*, Vol. 46, 1632–1639, Aug. 1999.

31. Plimmer, S. A., J. P. R. David, G. J. Rees, R. Grey, D. C. Herbert, D. R. Wright, and A. W. Higgs, "Impact ionization in thin $Al_xGa_{1-x}As$ ($x = 0.15$ and 0.30) $P^+ - I - N^+$ s," *J. Appl. Phys.*, Vol. 82, No. 3, 1231–1235, 1997.

32. Yuan, P., C. C. Hansing, K. A. Anselm, C. V. Lenox, H. Nie, A. L. Holmes Jr, B. G. Streetman, and J. C. Campbell, "Impact-ionization characteristics of III–V semiconductors for a wide range of multiplication region thicknesses," *IEEE J. Quantum Electron.*, Vol. 36, 198–204, 2000.

33. Saeid, M.-P., "Effect of change of multiplication region mole fraction on Characteristics of $Al_xGa_{1-x}As$-APDs in the linear and Geiger," *Progress In Electromagnetics Research B*, Vol. 2, 73–82, 2008.

34. Mokari, H. and M. H. Seyedi, "Numerical analysis of homojunc-

tion avalanche photodiodes (APDs)," *Progress In Electromagnetics Research C*, 2008 (accepted for publication).

35. Hayat, M. M., W. L. Sargeant, and B. E. A. Saleh, "Effect of dead space on gain and noise in Si and GaAs avalanche photodiodes," *IEEE J. Quantum Electron.*, Vol. 28, 1360–1365, 1992.

36. Hayat, M. M., Ü Sakŏlu, O.-H. Kwon, S. Wang, J. C. Campbell, B. E. A. Saleh, and M. C. Teich, "Breakdown probabilities for thin heterostructure avalanche photodiodes," *IEEE J. Quantum Electron.*, Vol. 39, 179–185, 2003.

37. McIntyre, R. J., "A new look at impact ionization — Part I: A theory of gain, noise, breakdown probability, and frequency response," *IEEE Trans. Electron Devices*, Vol. 46, 1623–1631, 1999.

38. Chen, Z.-H. and Q. Chu, "FDTD modeling of arbitrary linear lumped networks using piecewise linear recursive convolution technique," *Progress In Electromagnetics Research*, PIER 73, 327–341, 2007.

39. Hu, X.-J. and D.-B. Ge, "Study on conformal FDTD for electromagnetic scattering by targets with thin coating," *Progress In Electromagnetics Research*, PIER 79, 305–319, 2008.

40. Gong, Z. and G.-Q. Zhu, "FDTD analysis of an anisotropically coated missile," *Progress In Electromagnetics Research*, PIER 64, 69–80, 2006.

41. Xiao, S., B.-Z. Wang, P. Du, and Z. Shao, "An enhanced FDTD model for complex lumped circuits," *Progress In Electromagnetics Research*, PIER 76, 485–495, 2007.

42. Hu, X.-J. and D.-B. Ge, "Time domain analysis of active transmission line using FDTD technique," *Progress In Electromagnetics Research*, PIER 79, 305–319, 2008.

43. Chen, X., D. Liang, and K. Huang, "Microwave imaging 3-D buried objects using parallel genetic algorithm combined with FDTD technique," *Journal of Electromagnetic Waves and Applications*, Vol. 20, No. 13, 1471–1484, 2006.

44. Zheng, H.-X., X. -Q. Sheng, and E. K.-N. Yung, "Computation of scattering from conducting bodies coated with chiral materials using conformal FDTD," *Journal of Electromagnetic Waves and Applications*, Vol. 18, No. 11, 1761–1774, 2004.

45. Zhang, Y., W. Ding, and C. H. Liang, "Study on the optimum virtual topology for MPI based parallel conformal FDTD algorithm on PC clusters," *Journal of Electromagnetic Waves and Applications.*, Vol. 19, No. 13, 1817–1831, 2005.

46. Zheng, G., A. A. Kishk, A. W. Glisson, and A. B. Yakovlev, "A novel implementation of modified Maxwells equations in the periodic finite-difference time-domain method," *Progress In Electromagnetics Research*, PIER 59, 85–100, 2006.